Facilitation of Cognitive Performance and Reversal of the Effects of Sleep Deprivation by the Ampakine CX717 in Nonhuman Primates

Linda J. Porrino, James B. Daunais, Gary A. Rogers[1], Robert E. Hampson, Sam A. Deadwyler

Wake Forest University School of Medicine, Winston-Salem, NC
[1]Cortex Pharmaceuticals, Irvine, CA

Running Title – Ampakines reverse sleep deprivation

Number of Characters = 60,036 (limit 65,000)
Abstract = 152 words
Figures = 6
Tables = 1

Send Correspondence to:
Sam A Deadwyler, Ph.D.
Department of Physiology and Pharmacology
Wake Forest University Health Sciences
Medical Center Blvd.
Winston Salem, N.C. 27157-1083
Phone: 336-716-8540
FAX: 336-716-8501
E-mail: sdeadwyl@wfubmc.edu

Abstract

The ampakine CX717 (Cortex Pharmaceuticals, Irvine CA), a positive modulator of the glutamate AMPA receptor, was tested for its ability to enhance performance of a multi-object delayed matching to sample (DMS) task in monkeys and to reverse the effects of sleep deprivation on performance of the same task. CX717 dose-dependently enhanced performance under normal alert circumstances. Concomitant measures of regional brain glucose utilization (PET imaged $^{[18]}$F-Fluorodeoxyglucose) and single neuron activity in subjects performing the task showed that CX717 differentially and significantly enhanced activity in hippocampus and prefrontal cortex, both of which were selectively activated by the task under normal (nondrug) conditions. Prior administration of CX717 markedly reversed the effects of 30-36 hrs of sleep deprivation on task performance in the same monkeys. Consistent with this reversal, CX717 altered or reversed glucose utilization in brain regions showing the most disruption in sleep deprived animals, back to the pattern observed in normal alert conditions.

Introduction

The prevalence of glutamatergic synapses in the brain provides potent targets for the development of compounds to selectively enhance brain activity under both normal and compromised behavioral circumstances. Ampakines are positive modulators of the glutamatergic AMPA receptor subtype that are located on different types of neurons, and in nearly every brain region (Suppiramaniam et al., 2001). Ampakines have been shown to facilitate performance in several different behavioral testing paradigms in rodents (Staubli et al., 1994;Larson et al., 1995;Granger et al., 1996;Hampson et al., 1998b) and have been tested in humans (Marenco et al., 2002;Ingvar et al., 1997). These compounds have the potential to counteract the effects of disease, as well as enhance normal performance in cognitively challenging circumstances; however, such potential has not been realized to date (Ingvar et al., 1997).

In a recent study we described a process in the hippocampus which facilitates recognition memory by encoding objects with related features into distinct categories (Hampson et al., 2004), thereby increasing the capacity to remember stimuli in a delayed match to sample (DMS) paradigm without encoding the massive amounts of detail present in each new unique test item. Here we show that CX717 (Cortex Pharmaceuticals), an ampakine that facilitates AMPA receptor function, produces significant increases in DMS performance in normal alert monkeys and also counteracts the deleterious effects of 30-36 hours of sleep deprivation. A pharmacological basis for these findings is demonstrated via a significant relationship between the dose of CX717 and the compound's ability to enhance DMS performance. A neural basis is described in which differential actions are

present in brain regions activated during performance of the task. It is also demonstrated that CX717 counteracted or reversed the effects of sleep deprivation on cognition.

Results

The delayed match to sample (DMS) task is illustrated in Figure 1 and performance averaged over 8 different monkeys under normal alert conditions (with vehicle injection) is shown in Figure 2A. All animals showed delay-dependent performance accuracy, modified by the number of images (# images) presented in the Match phase of the task, as indicated by the difference between curves (overall ANOVA for effect of delay and images, $F_{(9,1391)} = 11.74$, $p<0.001$). Variability between animals and across trials was minimal ($F_{(1,1391)} = 1.61$, N.S.) and the linear nature of the relationship between delay and # images was consistent across all animals.

Figure 2B shows the effects of CX717 (0.8 mg/kg) on performance under normal alert conditions. Compared to vehicle sessions (Figure 2A), CX717 improved overall performance on the task by 15% (mean normal alert 75.0 ± 2.9 % vs. mean CX717 90.1 ± 1.3%, $F_{(1,1391)} = 15.72$, $p<0.001$). It is clear that there was a marked increase in % correct over all delays and # images, as illustrated by comparison using the dotted line with Figure 2A. This increase was most evident in the aspects of the task where performance was impaired the most in normal alert sessions: trials with delays of 21-30 sec and 5-6 images (mean normal alert: 47.1 ± 5.1% vs. mean CX717: 71.5 ± 2.5%; $F_{(1,1391)} = 24.92$, $p<0.001$). Figure 2C shows the effects of 30-36 hrs of sleep deprivation (SD) on performance of the DMS task. The effect of SD was to reduce overall DMS performance from the normal alert

condition by 12% (mean SD: 62.5 ± 2.4 %, $F_{(1,1391)} = 16.19$, $p<0.001$). It is obvious that performance was seriously affected (dotted line) as indicated by the effect of long delay trials with increased # images (21-30 sec, 5-6 images – mean normal alert: 47.1 ± 3.1% vs. mean SD: 36.0 ± 1.8%; $F_{(1,1391)} = 8.73$, $p<0.01$). However, the fact that performance was also significantly affected on trials with the shortest (1-10 sec) delays and the fewest (2-3) # images (mean normal alert: 96.1 ± 0.8% vs. mean SD: 85.7 ± 3.1%; $F_{(1,1391)} = 8.74$, $p<0.01$) suggests that the effects of SD were quite debilitating.

When CX717 (0.8 mg/kg) was administered 10 min before the sleep deprivation test session, the deleterious effects of 30-36 hours SD were markedly reduced and performance was restored back to its normal level. Figure 2D shows that DMS performance at all delays was enhanced over SD conditions (mean SD+CX717: 81.0 ± 2.2% vs. mean SD: 62.5 ± 2.4%; $F_{(1,1391)} = 17.46$, $p<0.001$) with even a trend toward improvement relative to the normal alert condition ($F_{(1,1391)} = 5.17$, $p<0.05$). Reversal by CX717 of the disruptive effects of SD on performance affected all delays and # images, with the most significant changes on trials with longer delays (21-30 sec) and increased # images (5-6) (mean SD+CX717: 60.6 ± 3.2% vs. mean SD: 37.7 ± 1.8%; $F_{(1,1391)} = 17.94$, $p<0.001$), indicating that the aspects of the task most severely affected by SD were the most improved by CX717 (dotted line in Figures 2C&D).

Figure 3A shows the dose-dependent facilitative effects of CX717 on normal alert DMS performance in individual sessions for each dose and monkey. Alternate daily sessions in which different doses of CX717 (dose range 0.3-1.5 mg/kg) were administered show the consistency across monkeys and the linear relationship between degree of

improvement and dosage. While daily performance in the task in normal alert session(s) ranged between 70-84% correct trials, performance on drug days (C, arrows) for CX717 doses over 0.5 mg/kg was > 81% correct. Doses of 0.8 and 1.5 mg/kg were highly effective (0.8 mg/kg, n=8, mean increase 12.2 ± 0.5%; $F_{(1,1391)} = 7.02$, $p<0.01$; 1.5 mg/kg, n=6, mean increase 15.1 ± 0.3%; $F_{(1,1391)} = 12.98$, $p<0.001$). Doses of 0.5 mg/kg (n=6) and lower were not as potent (mean increase 6.1±0.2%, $F_{(1,1391)} = 3.53$, N.S.). The specificity and selectivity of the effects of CX717 on performance was validated further by split session testing in which CX717 (0.8 mg/kg) was administered halfway through the session routinely in 4 animals. There was a marked improvement of 12.8 ± 0.5% in performance during the second half of the session ($F_{(1,1391)} > 13.91$, $p<0.001$).

Figures 3B&C show the effects of all four testing conditions segregated into the two main DMS task parameters of delay (B) and # images (C). Under normal alert conditions there was a systematic decrement in performance (Figure 3B circles) as a function of increase in delay, irrespective of # images (mean 1-5 sec: 94.6 ± 1.2% vs. mean 26-30 sec: 53.5 ± 3.8%, $F_{(5,1391)} = 9.24$, $p<0.001$). Correspondingly, increasing from 2 images to 6 images in the Match phase systematically reduced DMS performance, irrespective of delay (mean 2 images: 86.8 ± 4.1% vs. mean 6 images: 62.5 ± 6.1%, $F_{(4,1391)} = 4.93$, $p<0.001$). Figures 3B&C show that administration of CX717 (0.8 mg/kg, triangles) improved performance with respect to both parameters over normal alert conditions (Short to long delay, mean normal alert: 94.6-53.5% vs. mean CX717: 98.6-77.6%, $F_{(5,1391)} = 10.04$, $p<0.001$; # images 2 to 6, mean normal alert: 86.8-62.5% vs. mean CX717: 97.3-82.1%, $F_{(4,1391)} = 16.28$, $p<0.001$). From Figures 3B&C it is clear that SD (squares) produced a

highly significant impairment in these same parameters (Short to long delay, mean SD: 81.8-45.4%, $F_{(5,1391)} = 13.46$, $p<0.001$ vs. normal alert; # images, 2 to 6, mean SD: 74.7-48.8% vs. normal alert, $F_{(4,1391)} = 18.35$, $p<0.001$). Administration of CX717 (0.8mg/kg) reversed the effects of SD in a differential manner (Figures 3B&C, diamonds), showing marked increases across delays and # images in the SD condition (Short to long delay, mean SD+CX717: 93.5-67.3%, $F_{(5,1391)} = 15.89$, $p<0.001$ vs. SD; # images, 2 to 6, mean SD+CX717: 91.1-69.7%, $F_{(4,1391)} = 21.55$, $p<0.001$ vs. SD). In addition, when compared to normal alert sessions (Figures 3B&C circles), performance in the SD+CX717 condition was also slightly elevated (delay, $F_{(5,1391)} = 6.18$, $p<0.01$ vs. normal alert; # images, $F_{(4,1391)} = 5.64$, $p<0.01$ vs. normal alert) suggesting that CX717 may have improved performance above normal levels even in sleep deprived animals.

Figure 4A shows that CX717 and SD had marked but opposite effects on response latency during the task. The latencies to start the trial or respond to the Sample image were significantly reduced (gray bars) by CX717 at 0.8 mg/kg (Start trial: $F_{(1,1391)} = 10.17$, $p<0.001$; Sample: $F_{(1,1391)} = 7.48$, $p<0.01$; Match: $F_{(1,1391)} = 3.29$, N.S.). In contrast SD significantly increased (all $F_{(1,1391)} > 15.93$, $p<0.001$) response latencies in all 3 phases (diagonal-striped bars). The increase in response latency during SD did not reflect task interruption since the same mean number of trials was completed as in normal alert sessions. Consistent with the improved accuracy in performance, latencies in SD+CX717 sessions were substantially reduced (crosshatched bars) relative to SD sessions (all $F_{(1,1391)} > 17.14$, $p<0.001$) but not with respect to normal alert vehicle sessions ($F_{(1,1391)} = 1.93$, N.S.).

Figure 4B shows two examples of hippocampal cell firing correlates recorded during normal alert (left) and CX717 (right) sessions. The neurons qualified as "category cell types," recently shown by Hampson et al. (2004) to increase their discharge during the DMS task in response to images that could be classified similarly by common features which fit a particular category or class. The upper panels show that both neurons, recorded separately in their respective normal alert and CX717 sessions, showed the same "category" cell firing correlate (images of people), while the lower panels show lack of firing to examples of other images tested with similar visual elements (i.e. color, lines, etc.). Category neurons recorded during CX717 sessions (n=8) showed enhanced firing rates (Figure 4B upper) compared to those recorded in the normal alert sessions (normal alert: 14.6 ± 0.9 Hz; CX717: 20.2 ± 1.8, $F_{(1,209)} = 10.4$, $p<0.001$), indicating that CX717 directly influenced a hippocampal firing correlate presumably important for task performance (Hampson et al., 2004).

Figures 4C&D show the change in EEG recordings produced by sleep deprivation. There was a marked change in power spectral density (PSD) manifested as: 1) a shift toward higher power corresponding to the increase in lower frequency components (0.5-5 Hz), and 2) a specific increase in sleep spindles (18-26 Hz), in sleep deprived animals as they performed the task (Figure 4D, left and center). There was a high correlation between the above changes in PSD and decrements in behavioral performance (% correct) during sleep deprivation test sessions ($r^2 = 0.72$, $F_{(1,128)} = 9.94$, $p<0.01$). The most immediate indicator of the effects of CX717 on sleep deprived subjects was a rapid change in the EEG and PSD within 5-10 min following injection (0.8-1.5 mg/kg). This change was manifested

as a significant shift in PSD ($F_{(2,61)} = 6.17$, $p<0.01$) at the lower frequencies (0.5-5 Hz) and reduction in spindling (18-26 Hz) back toward normal alert conditions (Figure 4D, right).

Task-relevant Rates of Local Cerebral Glucose Utilization

Monkeys (n=6) were injected with ^{18}[F]-Fluorodeoxyglucose (FDG) 10 min prior to initiation of the DMS session. The isotope was incorporated for 45 min, while the animals continuously performed the task. They were then rapidly anesthetized and transported to the PET scanner for image acquisition. To identify regions in which task-relevant changes in brain activity occurred, it was necessary to obtain image data from FDG scans during a baseline non-task condition in which monkeys were chaired and habituated to presentation of the same video on 3 separate days for 45 min, then scanned on the 4th day after isotope incorporation during the 45 min. video presentation. These baseline scans were then subtracted from image data acquired during DMS task performance. Comparison with other conditions (i.e. CX717, SD) employed subtraction of the normal alert task scan. Rates of glucose metabolism ($ICMR_{glc}$) were assessed using regionalized values normalized by the global measures. A whole brain voxel-by-voxel analysis (SPM99) was conducted to identify those brain regions in which glucose utilization was increased or decreased by task performance. This was supplemented by an *a priori* region of interest (ROI) analysis of prefrontal cortex, hippocampus, parietal cortex and dorsal striatum, regions previously identified as involved in working memory tasks.

Table 1 summarizes the regions in which relative regional glucose metabolic rates ($ICMR_{glc}$) were altered during DMS performance under the normal alert, CX717, SD and

SD+CX717 conditions. Column 1 of the Table indicates that normal alert performance of the DMS task was associated with bilateral increases in $ICMR_{glc}$ in portions of the prefrontal cortex that included Broadmann's areas 46 (principal sulcus), 24, 9, 12, 45 and 47. Region of interest (ROI) analysis of these activated areas showed significant activations in left (t = 4.0; $p < .009$) and right hemispheres (t = 3.36; $p<0.017$) corrected for the ROI volume. $ICMR_{glc}$ was also increased under normal alert conditions bilaterally in the posterior hippocampus (Figure 5A left and middle). ROI analysis showed significant activations in left (t = 3.38; $p<0.033$) and right (t = 3.69; $p<0.036$) hippocampus corrected for ROI volume. Furthermore, additional regions of activations were found in dorsal striatum and within the posterior superior temporal gyrus (Table 1, col. 1). As a check on the reliability of these changes, strong activation was also observed in the primary and premotor cortices in the left hemisphere (reflecting the use of the right arm and hand in the task), and in the frontal eye fields (not shown). The patterns of change in $ICMR_{glc}$ shown in Table 1 were consistent in that very similar distributions of activation were obtained across all animals.

The effects of the administration of CX717 (0.8mg/kg) on $ICMR_{glc}$ during normal alert task performance are shown in the second column of Table 1. To identify the effects of CX717, image data obtained during normal alert DMS sessions were subtracted from data acquired in CX717 sessions. $ICMR_{glc}$ in hippocampus, prefrontal and parietal cortex was significantly increased by CX717 (Table 1). ROI analysis revealed significant activation in left (t = 3.3; $p < 0.01$) and right (t = 2.74; $p<0.015$) hippocampus, left (t = 4.48; $p<0.029$) and right (t = 4.73; $p<0.018$) parietal cortex and right (t = 3.21; $p < 0.038$) prefrontal cortex, each corrected for the volume of the ROI. Additional changes in metabolic rates were seen

in the ventral striatum (Figure 5A, right), left posterior cingulate, and right visual cortex (Table 1). In contrast, there was no further increase relative to the normal alert session in the dorsal striatum or superior temporal gyrus in the CX717 session.

Depriving the same animals of sleep for 30-36 hours produced differential changes in $ICMR_{glc}$ in specific brain regions concomitant with an overall decrease in task performance (Figure 2C). To identify those brain regions in which sleep deprivation altered cerebral metabolism during DMS performance, image data acquired during normal alert sessions were subtracted from data acquired during SD sessions. Table 1 (col. 3) shows that SD produced an increase in $ICMR_{glc}$ in the hippocampus relative to normal alert performance. An ROI analysis showed that increased glucose utilization was found in left (t = 4.09; $p<0.025$) and right (t = 4.05; $p<0.014$) hippocampus corrected for ROI volume. Increases were also evident bilaterally in the ventral striatum (Figure 5B middle and right), the posterior cingulate cortex, and portions of the visual cortex (areas V1, V2, and V4). $ICMR_{glc}$ however, was *decreased* in the prefrontal cortex relative to normal alert performance (Figure 5B left), as was the case in the dorsal striatum (Table 1). An ROI analysis of activity revealed significant decreases in both left (t = 3.44; $p<0.028$) and right (t = 3.16; $p<0.045$) prefrontal cortices and left dorsal striatum (t = 3.51; $p<0.019$) corrected for ROI volume. The thalamus, a region, that curiously did not show significant changes in $ICMR_{glc}$ under normal alert task conditions, exhibited a significant decrease following sleep deprivation (Table 1). The fact that these brain regions showed either significantly increased or decreased $ICMR_{glc}$ relative to the normal alert condition (Table 1) indicates that sleep deprivation either disrupted functional activity as in the prefrontal cortex, or

imposed additional metabolic demands on other regions (hippocampus and ventral striatum), in order to maintain even a moderate level of performance in the task (Figure , 2C).

Administration of CX717 to monkeys performing the DMS task after 30-36 hours of sleep deprivation *increased* $ICMR_{glc}$ in the prefrontal cortex (Table 1, col. 4) *compared to the decreases induced by sleep deprivation* (Figures 5B&C left). A similar reversal occurred in the dorsal striatum (Table 1). ROI analysis revealed significant increases in glucose utilization in left (t = 3.56; p<0.031) and right (t = 2.82; p<0.047) prefrontal cortex and in the right dorsal striatum (t = 3.56; p<0.048). However, in the ventral striatum the increases produced by sleep deprivation were reversed by administration of CX717, resulting in decreased $ICMR_{glc}$ during the task (Figure 5C right) as compared to $ICMR_{glc}$ during the SD sessions. In addition to these changes, activity increased in the right anterior superior temporal gyrus and right parietal cortex in sleep deprived animals given CX717 (Table 1). Thus, CX717 reversed the effects of sleep deprivation on task-relevant brain glucose utilization in several key brain regions in the same sessions in which there was significantly improved performance.

Multivariate Analyses of CX717 and Sleep Deprivation Effects on Cognition

Canonical linear discriminant analyses (Deadwyler et al., 1996;Hampson and Deadwyler, 1996;Deadwyler and Hampson, 1997) were used to examine the inter-relationships between performance of the DMS task and brain regions activated under the four treatment conditions. This type of multivariate analysis takes advantage of covariation

in different measures (% correct, response latency, changes in glucose utilization) at the single session and individual animal level, to extract relevant and significant sources of variance (discriminant functions, DFs) in relation to the four different test conditions (Stevens, 1992). The discriminant functions (DFs) were extracted from a covariance matrix formed by the following 12 measures: 1) % correct on all trials; 2) % correct on the most difficult trials (21-30 sec delay, 5-6 images); 3) % correct on the least difficult trials (1-10 sec delay, 2-3 images), 4) response latency to start the trial, 5) latency to Sample response, 6) latency to Match response, and 7-12) glucose utilization values from 6 different brain regions.

Figure 6A shows the three most significant sources of variance (discriminant functions, DFs) that contributed to the overall changes in each of the four experimental conditions. Means (± S.E.M.) of discriminant scores for each DF were averaged across monkeys, conditions, and trials, then plotted relative to a midpoint of zero indicating no influence of that DF. The most significant (highest) source of variance, DF1, represented changes in performance across the four test conditions. DF1 showed maximum variation when performance was markedly: 1) improved in the CX717 alone condition (normal alert score = -0.08; CX717 score = 3.89), or 2) impaired following sleep deprivation (SD score = 3.07, Figure 6A, red curve). The second most significant source of variance, DF2, was associated exclusively with the presence or absence of CX717. DF2 showed large negative scores (Figure 6A, green curve) when the drug was not present which then reversed to moderate positive values in sessions where the drug was administered. It is important to note that these changes had a similar profile to DF1 across the four conditions,

but were not differentially changed by either normal alert performance or sleep deprivation. The third most significant variance source, DF3, was associated with positive scores during the normal alert and CX717 conditions but exhibited negative scores whenever monkeys performed while sleep deprived (SD and SD+CX717), irrespective of the presence of CX717 (Figure 6A, blue curve). The three DFs therefore represented independent sources of variance operating to control behavior: a general performance related factor (DF1), a factor associated exclusively with CX717 irrespective of sleep deprivation (DF2), and a factor reflecting when animals were sleep deprived irrespective of performance changes or presence of CX717 (DF3).

In Figure 6B, each colored section of a bar reflects the degree of variance contributed by each DF to changes in a brain regional glucose utilization ($lCMR_{glc}$) score (entire bar) during one of the four test conditions. Positive scores reflect increases in relative $lCMR_{glc}$, and negative scores, decreases. It is clear that for most areas the effects of DF2 (green bars) were opposite those of DF3 (blue bars), showing predominately opposite score values for each DF in all conditions. In agreement with Table 1, Figure 6B shows that the thalamus and striatum were only minimally affected by DFs 1 and 2, but severely influenced by DF3 (sleep deprivation). In contrast, $lCMR_{glc}$ in parietal and prefrontal cortex as well as hippocampus was differentially altered by all three DFs (1, 2, and 3) across each of the four conditions. Finally, Figure 6B clearly shows that in the SD+CX717 condition, $lCMR_{glc}$ in 4 of 6 brain regions (except thalamus and cingulate cortex) had higher positive DF2 (green bars) scores relative to the SD only condition ($F_{(1,147)} = 11.40$, $p<0.001$). This was further supported by the fact that the markedly high

negative DF3 score in the thalamus during the SD-only condition (Figure 6B thalamus) was significantly reduced during the SD+CX717 condition ($F_{(1,147)} = 7.15$, $p<0.01$). The changes reflected in the CDA-ROI analysis are consistent with the results shown in Table 1 and indicate the degree to which each source of variance differentially affected regional changes in glucose utilization.

Discussion

The above findings support previous reports that ampakines improve cognitive performance in animals engaged in tasks the require working and short-term memory (Larson et al., 1995;Granger et al., 1996;Larson and Vanderklish, 1997;Hampson et al., 1998a;Hampson et al., 1998b). The degree to which performance was significantly enhanced in all 8 monkeys tested (Figure 3A) indicates that CX717 was quite potent, exhibiting a direct dose-effect relation to DMS performance. This enhanced performance by CX717 was also evidenced by significant increases in accuracy on the most difficult aspects of the task such as: 1) reducing the effects of longer delays (Figure 3B) as well as 2) the effects of increased # images (Figure 3C), In addition, Figure 6A shows that both performance (DF1) and drug (DF2) associated variances, even though separate, co-varied during all four testing conditions (red and green curves).

The marked deleterious effects on DMS performance of 30-36 hrs of sleep deprivation in these monkeys (Figures 2C and 3B&C) suggests an equivalence to effects of longer sleep deprivation episodes reported in human studies (Gillin et al., 2001;Caldwell et al., 2003;Wiegmann et al., 1996;Smith et al., 2002a). Other reports however, using more

subtle measures of cognitive function, provide evidence of severe effects of 36 hr sleep deprivation in young adults to the extent that performance was reduced to the level of non-sleep-deprived middle aged subjects (Harrison et al., 2000). Perhaps even more pertinent to the above findings are reports that deficits following sleep deprivation in humans were correlated with prefrontal-sensitive cognitive tasks (Anderson and Horne, 2003;Harrison et al., 2000). Our findings show that sleep deprivation produced highly significant performance deficits (Figures 2 and 3) and decreased prefrontal activation (Table 1, Figure 5B) in a task that increased prefrontal metabolic activity under normal alert conditions (Figure 5A). This was further substantiated by the fact that a significant source of variance in the study exclusively associated with sleep deprivation (DF3) contributed significantly to prefrontal glucose utilization (Figure 6B).

Another unique aspect of this study was the marked reversal by CX717 of the detrimental effects of 30-36 hrs of sleep deprivation on DMS performance in all 8 monkeys. Figures 2D and 3B&C show that the reversal in performance of sleep deprived animals was complete and even heightened somewhat relative to normal alert conditions, but remained below levels achieved when CX717 was given to non sleep-deprived animals (Figures 2B). This reversal was accompanied by changes in response latency (Figure 4A), as well as improved accuracy on trials with longer delays (Figure 3B) and increased # images (Figure 3C). Figure 6A shows a marked dissociation between DFs 1 & 2 and DF3 in the SD+CX717 condition suggesting that some behavioral processes sensitive to sleep deprivation may not have been altered by CX717. Thus, performance factors enhanced by CX717 under normal conditions were either: 1) reversed from their suppression by sleep

deprivation, or 2) enhanced to the same degree but were superimposed on an SD-depressed baseline (Figure 6A).

As a consequence of CX717 administration, brain glucose utilization in areas activated by the DMS task under normal alert conditions was increased in prefrontal and parietal cortices, ventral striatum and hippocampus (Table 1). The hippocampus and prefrontal cortex have been extensively implicated in working and short-term memory in monkeys and humans (Malkova and Mishkin, 2003;Wirth et al., 2003;Manns et al., 2003;Freedman et al., 2003;Freedman et al., 2001). Figure 4B indicates that the $ICMR_{glc}$ measures in hippocampus were reflections of increased neural activity associated with processing of information relevant to this particular version of DMS task (Hampson et al., 2004). Other brain regions shown in Table 1 that exhibited enhanced $ICMR_{glc}$ in the presence of CX717 included the ventral striatum and cingulate cortex, areas implicated in increased arousal and reward processes (Lauwereyns et al., 2002;Takikawa et al., 2002;Dudkin et al., 2003;Schultz et al., 1993). Finally, measures of covariation via CDA analysis (Figure 6B) confirmed the positive relationship between $ICMR_{glc}$ changes in these same brain regions and the significant elevation in performance by CX717 during those sessions.

The changes in $ICMR_{glc}$ produced by 30-36 hrs of sleep deprivation provide important clues as to which affected areas are vulnerable to reversals of performance by ampakines (Table 1). Two of the five structures normally engaged by the task (prefrontal cortex and dorsal striatum), showed significantly decreased $ICMR_{glc}$ following sleep deprivation, while the hippocampus showed a significant increase (Table 1). In addition, the

marked decrease in activation in the thalamus during SD was surprising since this structure did not show significant changes in either direction related to task or drug under normal alert conditions (Table 1). Finally, in contrast to prefrontal cortex, ventral striatum was the only structure to show significant decreased $ICMR_{glc}$ following sleep deprivation (Figure 5C). The above patterns were mirrored in the CDA analysis in which 4 of 6 brain areas exhibited large decreased $ICMR_{glc}$ changes associated with sleep deprivation that were opposite those generated during task performance under normal alert conditions (Figure 6B, SD, DF3).This suggests a tendency for CX717 to return the overall "pattern" of brain activation in sleep deprived animals to the same as that obtained during normal alert performance (Table 1, Figure 5C, SD+CX).

Because CX717 was effective in enhancing DMS performance under normal alert conditions, its reversal of the detrimental effects of sleep deprivation may result from a similar degree of effectiveness superimposed on the depressed performance baseline produced by sleep deprivation. Recent evidence strongly suggests that sleep deprivation may selectively down-regulate critical synaptic receptor mediated events in cortical neurons, compromising functional processes in many brain regions (Pace-Schott and Hobson, 2002;Meerlo et al., 2002;Shaffery et al., 2002;Siegel, 2001;Stickgold et al., 2001;Maquet, 2001;Johnson et al., 1999;Graves et al., 2001). The enhancement of AMPA receptor function in brain regions affected by sleep deprivation (Table 1) may compensate for these down-regulated systems provoked by SD (Graves et al., 2001;McDermott et al., 2003). Whether the effects of sleep deprivation on cognitive performance actually result from suppressed AMPA or other receptor processes is still in question (Smith and

Kennedy, 2003;Pace-Schott and Hobson, 2002;Meerlo et al., 2002). However, agents such as the ampakines which modulate many different glutamatergic pathways and circuits in separate brain regions (Danysz, 2002), could provide a basis for counteracting the cellular and synaptic changes that underlie deficits in cognitive performance that result from sleep deprivation in humans (Quigley et al., 2000;Drummond et al., 2000;Kingshott et al., 2000;Beaumont et al., 2001;Smith et al., 2002b;Thomas et al., 2000;Ferrara et al., 2000;Clark et al., 2001).

Other compounds that have been utilized to combat the effects of sleep deprivation, such as psychostimulants (amphetamine) and caffeine act through different (non-AMPA) neurotransmitter signaling pathways (Luca et al., 2000;Caldwell et al., 2003;Lieberman et al., 2002;Wesensten et al., 2002;Wiegmann et al., 1996;Landolt et al., 2000). The use of such drugs for this purpose, however, may be limited due to: 1) their potent stimulant actions which can distort cognitive and sensory processes at high doses, and 2) their addiction properties (Lieberman et al., 2002;Caldwell et al., 2003;Smith and Kennedy, 2003). The results presented here in nonhuman primates provide evidence that CX717 and possibly other members of the ampakine family may not only enhance cognitive performance under normal alert circumstances, but also ameliorate cognitive impairment in sleep deprived individuals.

Experimental Procedures

Behavioral Testing

Eight Rhesus macaque monkeys were utilized in the study. All animals were trained in a complex visual delayed-match-to-sample (DMS) task (Hampson et al., 2004) in which, after a 1-30 sec delay, images could vary in number from 2 to 6 in the Match phase of the task (Figure 1). Performance accuracy in choosing the sample image varied directly with 1) the number of images presented in the Match phase, and 2) duration of delay between the sample and match phase. Animals were tested daily on the task, during which they performed 150–300 trials per session. Stimuli consisted of large numbers of clip art images periodically obtained from the internet. No single clip art image was used for more than one trial during a single testing session. The ampakine CX717 (Cortex Pharmaceuticals) was administered in 10% w/v hydroxypropyl-beta-cyclodextrin and saline (0.45%) vehicle through an intravenous vascular access port to each monkey. CX717 was mixed as 1.5 mg/ml and administered within a dose range of 0.3 to 1.5 mg/kg to each monkey. On non-drug sessions, animals were given vehicle injections (cyclodextrin/saline) in the same manner. All monkeys were subjected to the sleep deprivation regimen which consisted of 30-36 hours of continuous observation and manipulations implemented by laboratory personnel that interfered with the animals' attempts to sleep overnight. Animals were maintained awake by showing them videos, playing music, feeding treats and gently shaking their cage and chair. During this time animals were housed in a continuously lighted room until the usual time of testing. EEG recordings were obtained in some animals during the sleep deprivation period and while testing.

Measurement of Brain Glucose Utilization

Brain glucose utilization measures were acquired via a General Electric (GE) Advance NXi PET scanner containing 18 rings of 672 4x8x30mm detectors each for a total of 12,096 detectors, providing 35 contiguous image planes with a 4.25 mm center-to-center spacing over a 15.2 cm axial field of view. The transaxial resolution of the scanner ranged from 3.8mm at the center of the field of view. Scanning consisted of a five minute transmission scan acquired in 2D mode using two rotating rod sources containing an equilibrium mixture of Ge-68/Ga-68. This was followed by a ten minute emission scan acquired in 3D mode (i.e. septa retracted). The image reconstruction of the 3D data used the 3D-reprojection method with full quantitative corrections. Transmission scan data was smoothed using a 4mm Gaussian filter transaxially and then segmented. The emission data was corrected for attenuation and reconstructed into 128 by 128 matrices using a Hanning filter with a 4mm cutoff transaxially and a ramp filter with an 8.5mm cutoff axially.

All animals were acclimated to experimental procedures, including blood collection, during the sessions prior to the initiation of the tests. On the day of the scan, animals were placed in primate chairs and the DMS task initiated. After 10 minutes of performance 3-5 mCi of [^{18}F]-2-deoxy-2-fluoro-D-glucose (FDG) was injected over 30 seconds. Blood samples were collected from the femoral vein (opposite the catheter) 8 minutes after infusion, a procedure which did not interfere with task performance. Animals performed the task for a total of 40 minutes after FDG administration, then the task was terminated and the animal rapidly anesthetized with ketamine (15 mg/kg, IV). A second blood sample was collected at 42 minutes and the animals transported to the scanner. Monkeys were

positioned in the scanner with reference to laser axes and scanning commenced. Following scan acquisition, monkeys were transported to their home cages and constantly monitored until fully recovered.

Tracer concentrations were measured in blood samples using an automated gamma well counter. A population-averaged FDG blood curve was scaled to each subject's measured blood curve for the time period from injection to the end of the PET scan (Takikawa et al., 1993). Data were transformed to glucose metabolic rates ($ICMR_{glc}$) based on the operational equation of (Sokoloff et al., 1977) as modified for monkeys by Kennedy et al (Kennedy et al., 1978) and by Phelps et al (Phelps et al., 1979) for human PET scans. Specifically, rate constants (k_1, k_2, and k_3) and lumped constant as determined in monkey by Kennedy (Kennedy et al., 1978), and used in quantitative autoradiographic 2-[^{14}C]deoxyglucose studies of monkeys (Sokoloff et al., 1977), were applied. In addition, a value for the rate constant, k_4, was applied because of the time of scan relative to injection of tracer. This value is that typically used in conscious, human adult PET scans (Phelps et al., 1979).

PET data were analyzed with Statistical Parametric Mapping (SPM99) software (Friston et al., 1995) implemented in MATLAB (MathWorks, Natick, MA). Reconstructed images were transformed into a standard space with an FDG template for rhesus monkeys constructed in our laboratory based on procedures of Black and colleagues (Black et al., 2001). Resultant images were smoothed using a 6mm isotropic Gaussian kernel. Global activity for each scan was proportionally scaled to a global mean of 55 μmol/100g/min.

Changes in cerebral glucose utilization were analyzed using the Multi subject: conditions and covariates option. The threshold for cluster size was set at 5 voxels and a statistical (f-test) threshold corresponding to $p<0.01$ (uncorrected for multiple comparisons) was employed. To identify the anatomical localization of activated areas, areas of activation were displayed on a T1 weighted anatomic MRI template available on the internet (Black et al., 2001) co-registered to the FDG template.

In addition, an *a priori* region of interest (ROI) analysis was conducted in prefrontal cortex, hippocampus, parietal cortex, and dorsal striatum based on previous imaging reports in non-human primates identifying these regions as involved in working memory tasks (Friedman and Goldman-Rakic, 1994;Inoue et al., 2004). ROIs were drawn on a structural MR template (Black et al., 2001) and were based on previous observations (Porrino et al., 2002). A second ROI analysis was conducted on the PET data for the multivariate analyses. For the latter analysis, 6 regions were chosen based on the results of the SPM analysis: prefrontal cortex, parietal cortex, striatum, thalamus, hippocampus, and cingulate cortex. Absolute rates of glucose utilization were determined bilaterally for each animal for each condition.

Acknowledgment: This research was supported by DARPA (ARO # 43278-LS) and NIH grants DA00119, DA06634 to S.A.D.; DA00414 to J.B.D. The authors thank Charles L. West, Ashley R. Morgan, Santos Ramirez, Christopher K. Craig, Mack Miller, Stephanie Rideout, Nancy Buchheimer, Kimberley Black, Holly Smith, Fred Fahey, and Lucy Fasano for technical assistance on the project.

References

Anderson C, Horne JA (2003) Prefrontal cortex: links between low frequency delta EEG in sleep and neuropsychological performance in healthy, older people. Psychophysiology 40: 349-357.

Beaumont M, Batejat D, Pierard C, Coste O, Doireau P, Van Beers P, Chauffard F, Chassard D, Enslen M, Denis JB, Lagarde D (2001) Slow release caffeine and prolonged (64-h) continuous wakefulness: effects on vigilance and cognitive performance. J Sleep Res 10: 265-276.

Black KJ, Koller JM, Snyder AZ, Perlmutter JS (2001) Template images for nonhuman primate neuroimaging: 2. Macaque. Neuroimage 14: 744-748.

Caldwell JL, Prazinko BF, Rowe T, Norman D, Hall KK, Caldwell JA (2003) Improving daytime sleep with temazepam as a countermeasure for shift lag. Aviat Space Environ Med 74: 153-163.

Clark CP, Frank LR, Brown GG (2001) Sleep deprivation, EEG, and functional MRI in depression: preliminary results. Neuropsychopharmacology 25: S79-S84.

Danysz W (2002) CX-516 Cortex pharmaceuticals. Curr Opin Investig Drugs 3: 1081-1088.

Deadwyler SA, Bunn T, Hampson RE (1996) Hippocampal ensemble activity during spatial delayed-nonmatch-to-sample performance in rats. J Neurosci 16: 354-372.

Deadwyler SA, Hampson RE (1997) The significance of neural ensemble codes during behavior and cognition. In: Annual Review of Neuroscience, Vol. 20 (Cowan WM, Shooter EM, Stevens CF, Thompson RF, eds), pp 217-244. Palo Alto, CA: Annual Reviews, Inc.

Drummond SP, Brown GG, Gillin JC, Stricker JL, Wong EC, Buxton RB (2000) Altered brain response to verbal learning following sleep deprivation. Nature 403: 655-657.

Dudkin KN, Chueva IV, Arinbasarov MU, Bobkova NV (2003) Organization of working memory processes in monkeys: the effects of a dopamine receptor agonist. Neurosci Behav Physiol 33: 387-398.

Ferrara M, De Gennaro L, Casagrande M, Bertini M (2000) Selective slow-wave sleep deprivation and time-of-night effects on cognitive performance upon awakening. Psychophysiology 37: 440-446.

Freedman DJ, Riesenhuber M, Poggio T, Miller EK (2001) Categorical representation of visual stimuli in the primate prefrontal cortex. Science 291: 312-316.

Freedman DJ, Riesenhuber M, Poggio T, Miller EK (2003) A comparison of primate prefrontal and iTemporal cortices during visual categorization. J Neurosci 23: 5235-5246.

Friedman HR, Goldman-Rakic PS (1994) Coactivation of prefrontal cortex and inferior parietal cortex in working memory tasks revealed by 2DG functional mapping in the rhesus monkey. J Neurosci 14: 2775-2788.

Friston KJ, Holmes AP, Worsley KJ, Poline JP, Frith CD, Frackowiak RSJ (1995) Statistical parametric maps in functional imaging: A genreral linear approach. Human Brain Mapping 2: 189-210.

Gillin JC, Buchsbaum M, Wu J, Clark C, Bunney W, Jr. (2001) Sleep deprivation as a model experimental antidepressant treatment: findings from functional brain imaging. Depress Anxiety 14: 37-49.

Granger R, Deadwyler SA, Davis M, Moskovitz B, Kessler M, Rogers G, Lynch G (1996) Facilitation of glutamate receptors reverses an age-associated memory impairment in rats. Synapse 22: 332-337.

Graves L, Pack A, Abel T (2001) Sleep and memory: a molecular perspective. Trends Neurosci 24: 237-243.

Hampson RE, Deadwyler SA (1996) Ensemble codes involving hippocampal neurons are at risk during delayed performance tests. Proc Natl Acad Sci U S A 93: 13487-13493.

Hampson RE, Pons TP, Stanford TR, Deadwyler SA (2004) Categorization in the monkey hippocampus: A possible mechanism for encoding information into memory. Proc Natl Acad Sci U S A 101: 3184-3189.

Hampson RE, Rogers G, Lynch G, Deadwyler SA (1998a) Facilitative effects of the ampakine CX516 on short-term memory in rats: Correlations with hippocampal ensemble activity. J Neurosci 18: 2748-2763.

Hampson RE, Rogers G, Lynch G, Deadwyler SA (1998b) Facilitative effects of the ampakine CX516 on short-term memory in rats: Enhancement of delayed-nonmatch-to-sample performance. J Neurosci 18: 2740-2747.

Harrison Y, Horne JA, Rothwell A (2000) Prefrontal neuropsychological effects of sleep deprivation in young adults--a model for healthy aging? Sleep 23: 1067-1073.

Ingvar M, Ambros-Ingerson J, Davis M, Granger R, Kessler M, Rogers GA, Schehr RS, Lynch G (1997) Enhancement by an ampakine of memory encoding in humans. Exp Neurol 146: 553-559.

Inoue M, Mikami A, Ando I, Tsukada H (2004) Functional brain mapping of the macaque related to spatial working memory as revealed by PET. Cereb Cortex 14: 106-119.

Johnson SA, Luu NT, Herbst TA, Knapp R, Lutz D, Arai A, Rogers GA, Lynch G (1999) Synergistic interactions between ampakines and antipsychotic drugs. J Pharmacol Exp Ther 289: 392-397.

Kennedy C, Sakurada O, Shinohara M, Jehle J, Sokoloff L (1978) Local cerebral glucose utilization in the normal conscious macaque monkey. Ann Neurol 4: 293-301.

Kingshott RN, Cosway RJ, Deary IJ, Douglas NJ (2000) The effect of sleep fragmentation on cognitive processing using computerized topographic brain mapping. J Sleep Res 9: 353-357.

Landolt HP, Finelli LA, Roth C, Buck A, Achermann P, Borbely AA (2000) Zolpidem and sleep deprivation: different effect on EEG power spectra. J Sleep Res 9: 175-183.

Larson J, Lieu T, Petchpradub V, LeDuc B, Ngo H, Rogers GA, Lynch G (1995) Facilitation of olfactory learning by a modulator of AMPA receptors. J Neurosci 15: 8023-8030.

Larson J, Vanderklish PW (1997) Involvement of AMPA receptors in LTP mechanisms and memory. In: Long-Term Potentiation, Volume 3 (Baudry M, Davis JL, eds), pp 73-104. Cambridge,MA: MIT Press.

Lauwereyns J, Takikawa Y, Kawagoe R, Kobayashi S, Koizumi M, Coe B, Sakagami M, Hikosaka O (2002) Feature-based anticipation of cues that predict reward in monkey caudate nucleus. Neuron 33: 463-473.

Lieberman HR, Tharion WJ, Shukitt-Hale B, Speckman KL, Tulley R (2002) Effects of caffeine, sleep loss, and stress on cognitive performance and mood during U.S. Navy SEAL training. Sea-Air-Land. Psychopharmacology (Berl) 164: 250-261.

Luca AF, Hans-Peter L, Alfred B, Corinne R, Thomas B, Alexander AB, Peter A (2000) Functional neuroanatomy of human sleep states after zolpidem and placebo: A H215O-PET study. Journal of Sleep Research 9: 161-173.

Malkova L, Mishkin M (2003) One-trial memory for object-place associations after separate lesions of hippocampus and posterior parahippocampal region in the monkey. J Neurosci 23: 1956-1965.

Manns JR, Hopkins RO, Reed JM, Kitchener EG, Squire LR (2003) Recognition memory and the human hippocampus. Neuron 37: 171-180.

Maquet P (2001) The role of sleep in learning and memory. Science 294: 1048-1052.

Marenco S, Egan MF, Goldberg TE, Knable MB, McClure RK, Winterer G, Weinberger DR (2002) Preliminary experience with an ampakine (CX516) as a single agent for the treatment of schizophrenia: a case series. Schizophr Res 57: 221-226.

McDermott CM, LaHoste GJ, Chen C, Musto A, Bazan NG, Magee JC (2003) Sleep deprivation causes behavioral, synaptic, and membrane excitability alterations in hippocampal neurons. J Neurosci 23: 9687-9695.

Meerlo P, Koehl M, van der Borght K, Turek FW (2002) Sleep restriction alters the hypothalamic-pituitary-adrenal response to stress. J Neuroendocrinol 14: 397-402.

Pace-Schott EF, Hobson JA (2002) The neurobiology of sleep: genetics, cellular physiology and subcortical networks. Nat Rev Neurosci 3: 591-605.

Phelps ME, Huang SC, Hoffman EJ, Selin C, Sokoloff L, Kuhl DE (1979) Tomographic measurement of local cerebral glucose metabolic rate in humans with (F-18)2-fluoro-2-deoxy-D-glucose: validation of method. Ann Neurol 6: 371-388.

Porrino LJ, Lyons D, Miller MD, Smith HR, Friedman DP, Daunais JB, Nader MA (2002) Metabolic mapping of the effects of cocaine during the initial phases of self-administration in the nonhuman primate. J Neurosci 22: 7687-7694.

Quigley N, Green JF, Morgan D, Idzikowski C, King DJ (2000) The effect of sleep deprivation on memory and psychomotor function in healthy volunteers. Hum Psychopharmacol 15: 171-177.

Schultz W, Apicella P, Ljungberg T (1993) Responses of monkey dopamine neurons to reward and conditioned stimuli during successive steps of learning a delayed response task. J Neurosci 13: 900-913.

Shaffery JP, Sinton CM, Bissette G, Roffwarg HP, Marks GA (2002) Rapid eye movement sleep deprivation modifies expression of long-term potentiation in visual cortex of immature rats. Neuroscience 110: 431-443.

Siegel JM (2001) The REM sleep-memory consolidation hypothesis. Science 294: 1058-1063.

Smith GS, Reynolds CF, III, Houck PR, Dew MA, Ma Y, Mulsant BH, Pollock BG (2002a) Glucose metabolic response to total sleep deprivation, recovery sleep, and acute antidepressant treatment as functional neuroanatomic correlates of treatment outcome in geriatric depression. Am J Geriatr Psychiatry 10: 561-567.

Smith ME, McEvoy LK, Gevins A (2002b) The impact of moderate sleep loss on neurophysiologic signals during working-memory task performance. Sleep 25: 784-794.

Smith RL, Kennedy CH (2003) Increases in avoidance responding produced by REM sleep deprivation or serotonin depletion are reversed by administration of 5-hydroxytryptophan. Behav Brain Res 140: 81-86.

Sokoloff L, Reivich M, Kennedy C, Des Rosiers MH, Patlak CS, Pettigrew KD, Sakurada O, Shinohara M (1977) The [14C]deoxyglucose method for the measurement of local cerebral glucose utilization: theory, procedure, and normal values in the conscious and anesthetized albino rat. J Neurochem 28: 897-916.

Staubli U, Perez Y, Xu F-B, Rogers G, Ingvar M, Stone-Elander S, Lynch G (1994) Centrally active modulators of glutamate receptors facilitate the induction of long-term potentiation in vivo. Proc Natl Acad Sci U S A 91: 11158-11162.

Stevens J (1992) Applied Multivariate Statistics for the Social Sciences. Hillsdale: Lawrence Erlbaum Associates.

Stickgold R, Hobson JA, Fosse R, Fosse M (2001) Sleep, learning, and dreams: off-line memory reprocessing. Science 294: 1052-1057.

Suppiramaniam V, Bahr BA, Sinnarajah S, Owens K, Rogers G, Yilma S, Vodyanoy V (2001) Member of the Ampakine class of memory enhancers prolongs the single channel open time of reconstituted AMPA receptors. Synapse 40: 154-158.

Takikawa S, Dhawan V, Spetsieris P, Robeson W, Chaly T, Dahl R, Margouleff D, Eidelberg D (1993) Noninvasive quantitative fluorodeoxyglucose PET studies with an estimated input function derived from a population-based arterial blood curve. Radiology 188: 131-136.

Takikawa Y, Kawagoe R, Hikosaka O (2002) Reward-dependent spatial selectivity of anticipatory activity in monkey caudate neurons. J Neurophysiol 87: 508-515.

Thomas M, Sing H, Belenky G, Holcomb H, Mayberg H, Dannals R, Wagner H, Thorne D, Popp K, Rowland L, Welsh A, Balwinski S, Redmond D (2000) Neural basis of alertness and cognitive performance impairments during sleepiness. I. Effects of 24 h of sleep deprivation on waking human regional brain activity. J Sleep Res 9: 335-352.

Wesensten NJ, Belenky G, Kautz MA, Thorne DR, Reichardt RM, Balkin TJ (2002) Maintaining alertness and performance during sleep deprivation: modafinil versus caffeine. Psychopharmacology (Berl) 159: 238-247.

Wiegmann DA, Stanny RR, McKay DL, Neri DF, McCardie AH (1996) Methamphetamine effects on cognitive processing during extended wakefulness. Int J Aviat Psychol 6: 379-397.

Wirth S, Yanike M, Frank LM, Smith AC, Brown EN, Suzuki WA (2003) Single neurons in the monkey hippocampus and learning of new associations. Science 300: 1578-1581.

Figure Legends:

Figure 1: Multi-image visual delayed-match-to-sample (DMS) task. **Top:** Stages of a DMS trial. (1) Start trial display (circle) for initiation of trial; (2) Presentation of Sample image ("hand pushing button"); (3) Interposed Delay (1-30 sec), screen blanked. (4) Match phase presentation of Sample image ("hand") plus up to five possible nonmatch images (e.g. "shell" and "deer", see also below). **Bottom:** Examples of Sample image (left) and a selection of images including the Sample that would appear in the Match phase of a DMS trial (center). Each trial-specific Sample image was presented to the monkey in a random location on the computer screen. The monkey was required to respond and place the cursor in the image to continue the trial. The screen was blanked for 1-30 sec before the presentation of multiple images (2-6) in the Match phase at random screen locations with the Sample image always in a different location from its prior position. Images in the Match phase, other than the Sample image, varied in color, shape and content (B) and were also only used once per session. Selection of the Sample image (asterisk) in the Match phase was rewarded with juice and terminated the trial. If the cursor touched another (nonmatch) image for more than 200 ms the trial was terminated with no reward. There was 10 sec between each trial in which the screen was blank.

Figure 2: Effects of CX717 and sleep deprivation on performance in DMS task. **A.** Normal alert vehicle sessions showing mean (± SEM) % correct trials for DMS performance averaged over 8 different monkeys. Each curve reflects performance for trials sorted by number (#) of images (2-6) and different delays (1-30 sec in 5 sec increments). Performance decreased as a function of delay duration and # images as indicated by separation in the 5 curves. Arrow and "C" indicate random "chance" performance with respect to % Correct trials. **B.** Enhanced DMS performance by same monkeys when

CX717 (0.8 mg/kg) was administered 10 min prior to session. Performance with respect to # images (different curves) and duration of delay (as in A) was maximally facilitated as indicated by comparison to dotted reference line at 60% in A and B. **C.** Mean (±SEM) % correct DMS performance, with the same trial protocol, in sessions following 30–36 hours of sleep deprivation. Dotted line allows comparison at 60% of performance level with A and B above. **D.** Reversal of effects of sleep deprivation on DMS performance by prior administration of CX717 (0.8 mg/kg) in same 8 monkeys. Dotted line across graph provides comparison with sleep deprivation (C) and vehicle sessions (A).

Figure 3: Partitioning of DMS performance by dose, delay and number of images. **A.** Effects of CX717 on average performance over single sessions (per monkey, summed over all trials per session) for 3 different dose ranges (0.3-0.5, 0.8-1.0 and 1.5 mg/kg) interspersed with vehicle sessions. Individual monkeys designated by different symbols at right. Arrows indicate CX717 (C) sessions. **B.** Partitioning of DMS performance by delay plotted for normal alert, CX717, SD, SD+CX717 conditions. Mean (± SEM) % correct for 1–30 sec delays summed over 2-6 image trials. Each curve represents one condition. Arrow and "C" on axis indicate "chance" performance level in task as in Fig. 2. **C.** DMS performance in each of the trials conditions partitioned by # images (summed over different delays). CX717 (0.8 mg/kg) was administered prior to each session in the CX717 and SD+CX717 conditions. Legend as in B.

Figure 4: **A.** Response latency (mean sec ± SEM) for Start trial, Sample and Match phases of task. Effects of sleep deprivation (diagonal-striped bars) and reversal by CX717 (0.8 mg/kg) on latency to respond (cross-hatched bars) are shown with normal alert and

CX717 conditions. Latency (mean sec ± SEM) was calculated as temporal difference between image appearance on the screen and cursor entry into image. Data from same sessions shown in Figures 2 and 3. Start trial, Sample and Match Phase responses shown. **B.** Extracellular single cell recordings of action potentials from two different hippocampal neurons characterized as "category cells" (Hampson et al., 2004) during normal alert (left) and CX717 (right) sessions in the same monkey. Left: Perievent raster and histogram showing firing of hippocampal cell (individual "dots") in Sample phase of task in normal alert session. Raster shows 20 consecutive trials (each row of dots = 1 trial) above normalized perievent histogram (bin width = 250 ms) which is summed firing over 150 trial session. Top shows increased firing to images from "people" category; bottom shows lack of firing increase to images that are not "people." Images presented (Pres.) at solid vertical line in raster/histogram display. Right: Raster and histogram show increased firing for a neuron recorded in CX717 (1.5 mg/kg) session responsive to same types of images (i.e. containing people) as the one recorded in vehicle session. **C.** Individual monkey EEG recorded from six different electrode locations on surface of parietal and occipital cortex in normal alert (top) and sleep-deprived (bottom) sessions. Different frequencies indicated by superimposed sine waves. **D.** Average power spectral density (PSD) plots show increase in occurrence of high amplitude slow waves (0.5-5 Hz, above dotted line) and "sleep spindles" (18-26 Hz, asterisks) in EEG (left) following sleep deprivation (middle). Reversal of sleep deprivation (right) by CX717 (0.8 mg/kg) indicated by decrease in PSD at frequencies 0.5-5 Hz (dotted line) and reduction in spindles (asterisk). PSDs calculated as log of root-mean-square power in 10 min EEG recordings,

using frequency increments of 0.25 Hz, averaged over four monkeys in each condition indicated.

Figure 5: Composite SPM derived PET images of brain glucose utilization ($ICMR_{glc}$) constructed from 6 monkeys during performance of DMS task. **A.** Top row shows example of two brain regions (prefrontal cortex-left and hippocampus-middle) that exhibited largest increases in $ICMR_{glc}$ during performance of DMS task compared to baseline no-task condition (Table 1, column 1). SPM derived PET values shown co-registered with representative MRI template in sagittal plane as colored squares (voxels). Rates of glucose utilization ($ICMR_{glc}$) were normalized across 6 different monkeys. Image at right shows increase in ventral striatum following administration of CX717 (0.8 mg/kg) relative to normal alert condition. Similar changes occurred in hippocampus and prefrontal cortex (Table 1, column 2). **B.** Middle row shows effects of sleep deprivation (30–36 hrs) on SPM derived $ICMR_{glc}$ images during performance of DMS task. Prefrontal cortex (left) shows decreased $ICMR_{glc}$, while hippocampus (middle) and ventral striatum/cingulate cortex (right) showed increases in $ICMR_{glc}$ relative to normal alert session. **C.** Bottom row shows effect of CX717 (0.8 mg/kg) on sleep deprived $ICMR_{glc}$ measures. Prefrontal cortex (left) shows increased $ICMR_{glc}$ during performance of task *relative to sleep deprived session* (B). Ventral striatum (right) exhibited reduced $ICMR_{glc}$ in SD+CX717 (0.8 mg/kg) condition *relative to sleep deprived session* (B). Middle is blank because hippocampus showed no change from sleep deprived status (B) in SD+CX717 condition. Color scale for increased $ICMR_{glc}$ is $p<0.05$ (red) for student's t-test. Voxel (colored squares) size = 2 mm. Brain areas as labeled.

Figure 6: Multivariate canonical discriminant analysis (CDA) of overall DMS performance and brain glucose utilization for 6 monkeys across all four behavioral conditions. Discriminant functions (DFs 1,2,3) were extracted via CDA from multidimensional space formed by the following measures: % correct on all trials; % correct on "difficult" trials (21-30 sec delays, 5-6 images); % correct on "simple" trials (1-10 sec delays, 2-3 images); response latencies for start trial, sample and match phase; and $ROI/ICMR_{glc}$ measures from 6 different brain regions in each monkey. DFs 1, 2, 3 constitute the respectively ranked sources of variance extracted across the four conditions labeled: normal alert, CX717 (0.8 mg/kg), SD (sleep deprived) and SD+CX717. **A.** Discriminant scores (DMS performance measures weighted by normalized coefficients from the CDA) were generated for each animal and session, and plotted as means (± SEM) for each DF (different colors) within the four behavioral conditions. Score magnitudes were normalized to mean=0, std. dev.=1 and orthogonally rotated such that positive indicates increased performance accuracy and a corresponding decrease in response latency. **B.** Above CDA analysis was used to extract sources of variance associated with changes in $ICMR_{glc}$ based on region of interest (ROI) assessments. DF 1, 2 and 3 coefficient weightings of $ICMR_{glc}$ within 6 different brain regions, identified in the ROI, were determined over the same four behavioral conditions as in A. The length of each colored bar indicates the relative contribution of the respective DF to the change in $ICMR_{glc}$ within a brain region for a given condition. Positive values indicate relative changes $ICMR_{glc}$ with respect to "0" (the mean level of glucose utilization across all 6 brain areas in each monkey). Negative scores indicate relative decreases in $ICMR_{glc}$ within a brain region.

Fig 1

DMS Trials Consist of Clip-Art Images

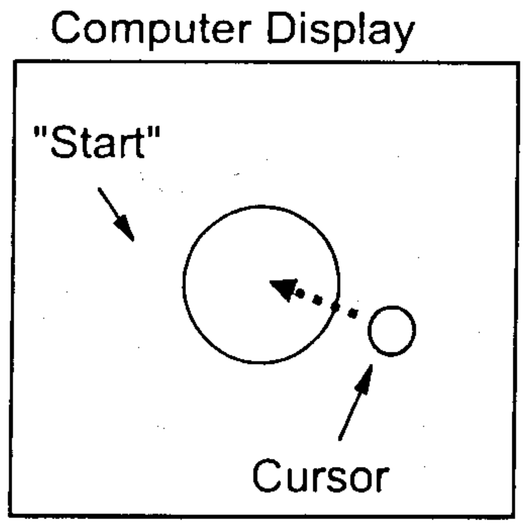

Start trial: Monkey places cursor in ring.

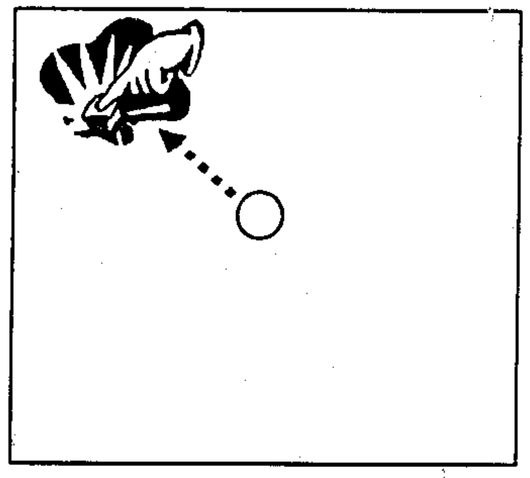

Sample Phase: Single image presented

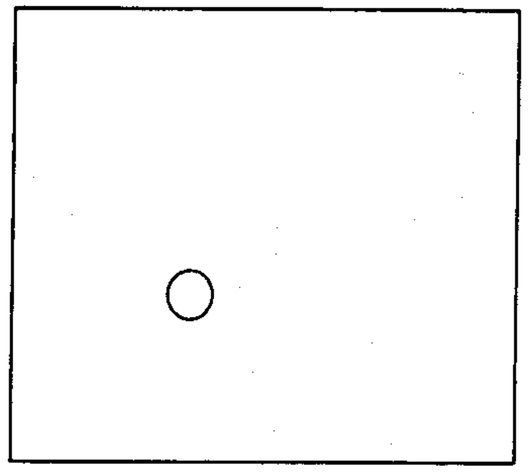

Delay Phase: 1-30 sec., blank screen

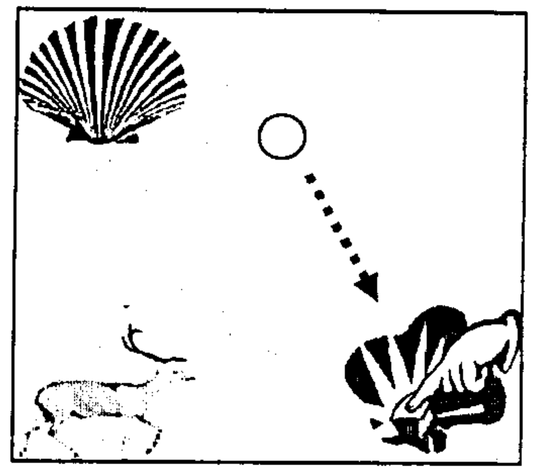

Match Phase: Select same image

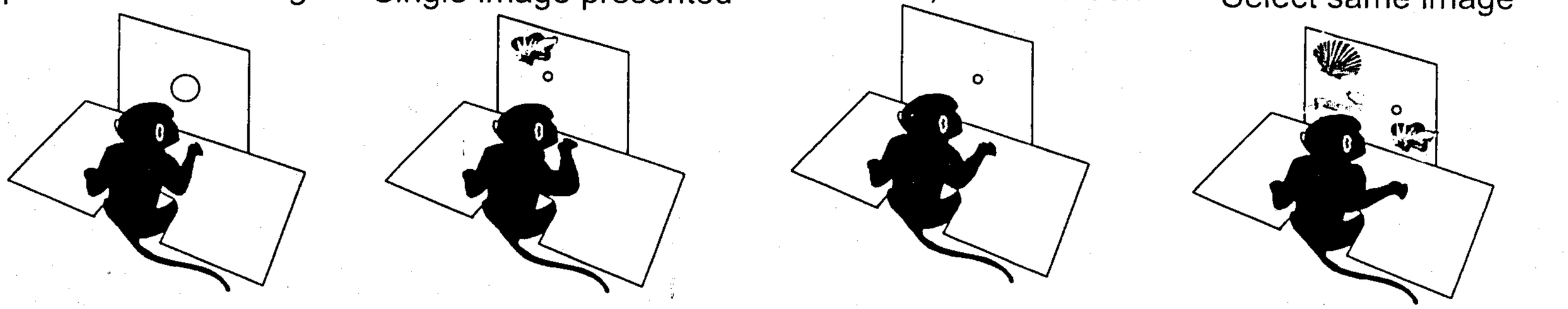

Sample Image

Match Phase Images

Trial 1			 *	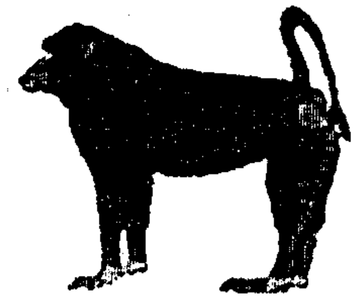		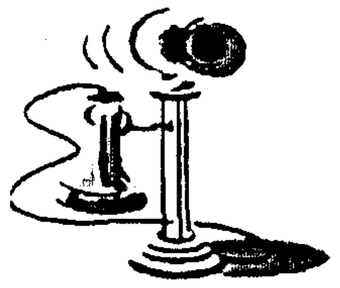
Trial 2			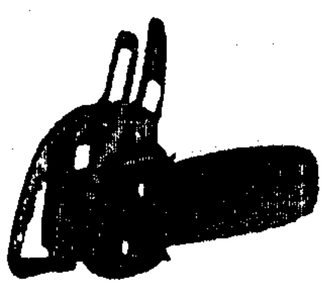	 *	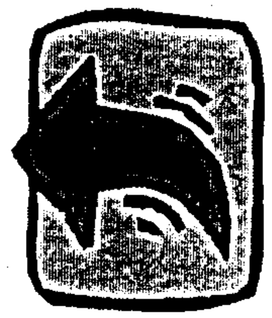	

* Correct Response

Fig 2

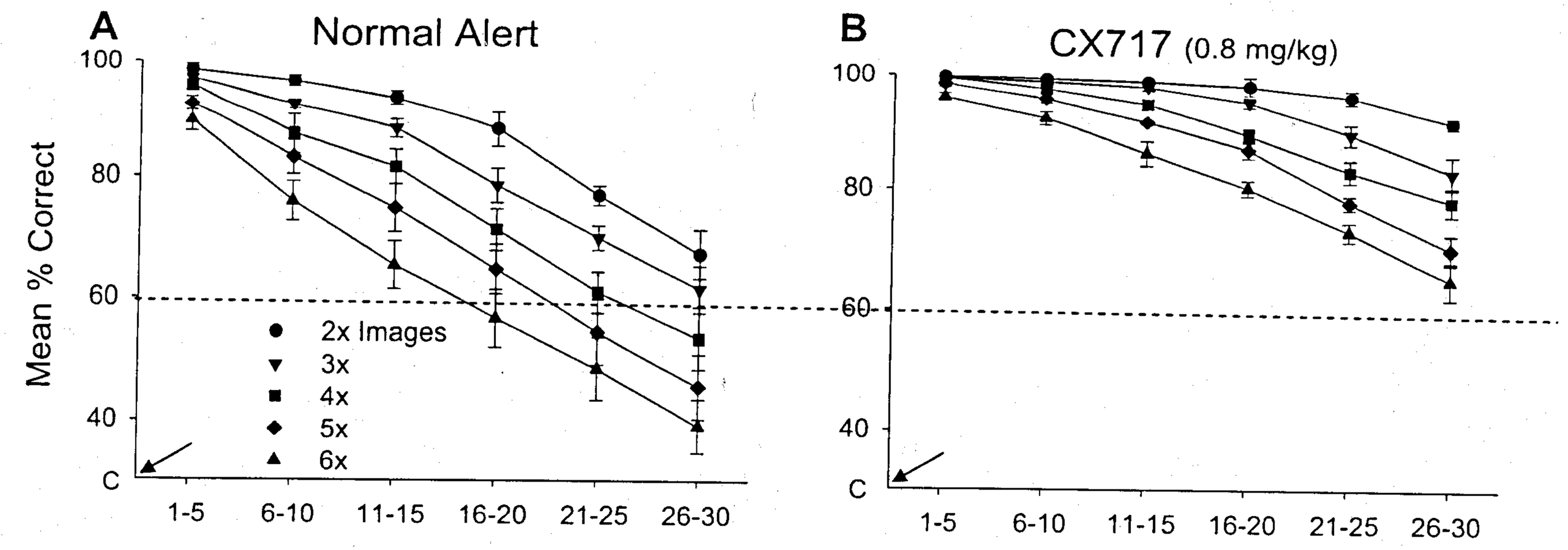
A
Normal Alert
B
CX717 (0.8 mg/kg)
Mean % Correct
100
80
60
40
C
2x Images
3x
4x
5x
6x
1-5
6-10
11-15
16-20
21-25
26-30
C
Sleep Deprived
D
SD+CX717 (0.8 mg/kg)
Delay (sec)

Fig 3

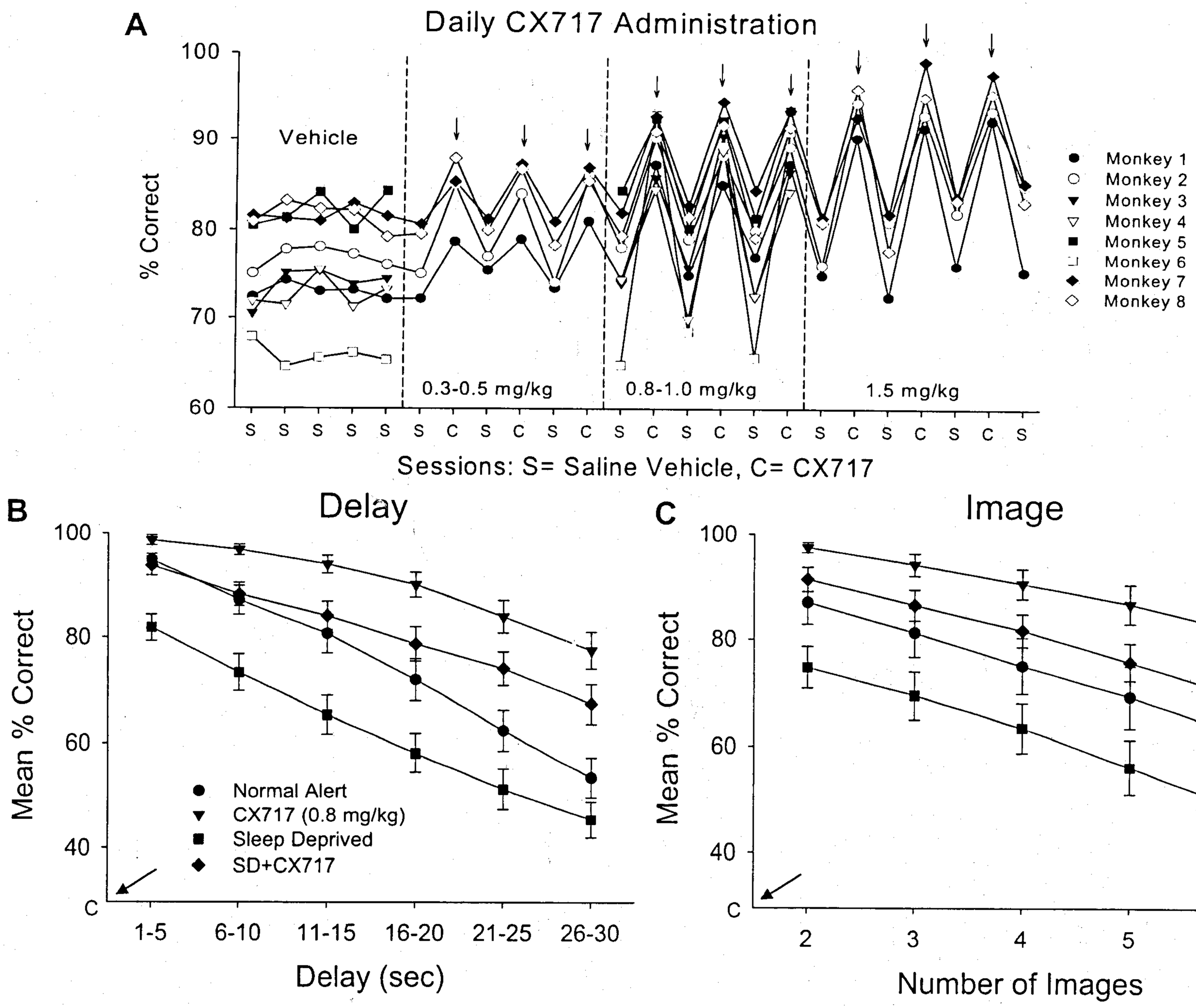
A
Daily CX717 Administration
% Correct
100
90
80
70
60
Vehicle
0.3-0.5 mg/kg
0.8-1.0 mg/kg
1.5 mg/kg
S S S S S S C S C S C S C S C S C S C S C S C S
Sessions: S= Saline Vehicle, C= CX717
Monkey 1
Monkey 2
Monkey 3
Monkey 4
Monkey 5
Monkey 6
Monkey 7
Monkey 8
B
Delay
Mean % Correct
100
80
60
40
C
Normal Alert
CX717 (0.8 mg/kg)
Sleep Deprived
SD+CX717
1-5
6-10
11-15
16-20
21-25
26-30
Delay (sec)
C
Image
Mean % Correct
100
80
60
40
C
2
3
4
5
6
Number of Images

Fig 4

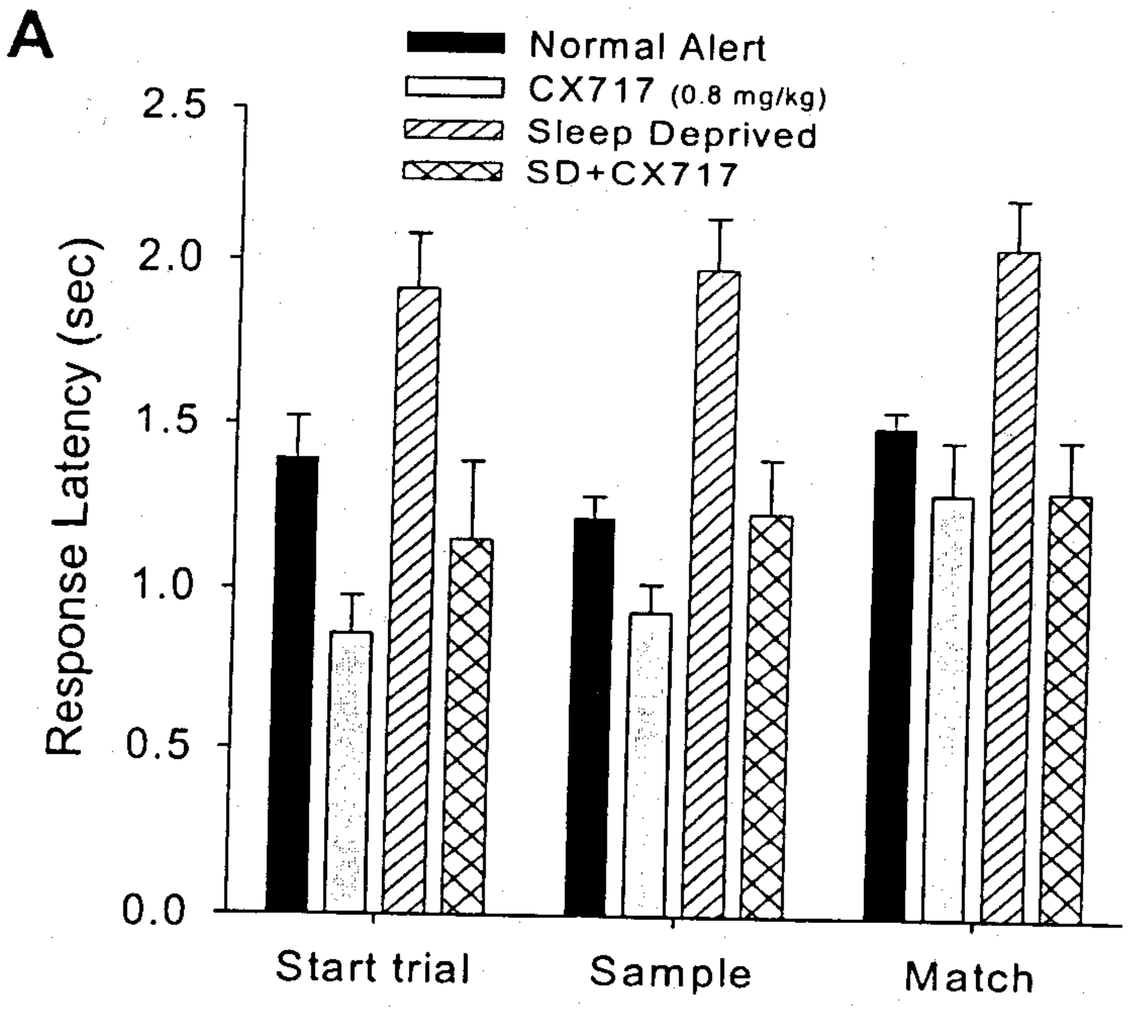
A
Normal Alert
CX717 (0.8 mg/kg)
Sleep Deprived
SD+CX717
Response Latency (sec)
2.5
2.0
1.5
1.0
0.5
0.0
Start trial
Sample
Match

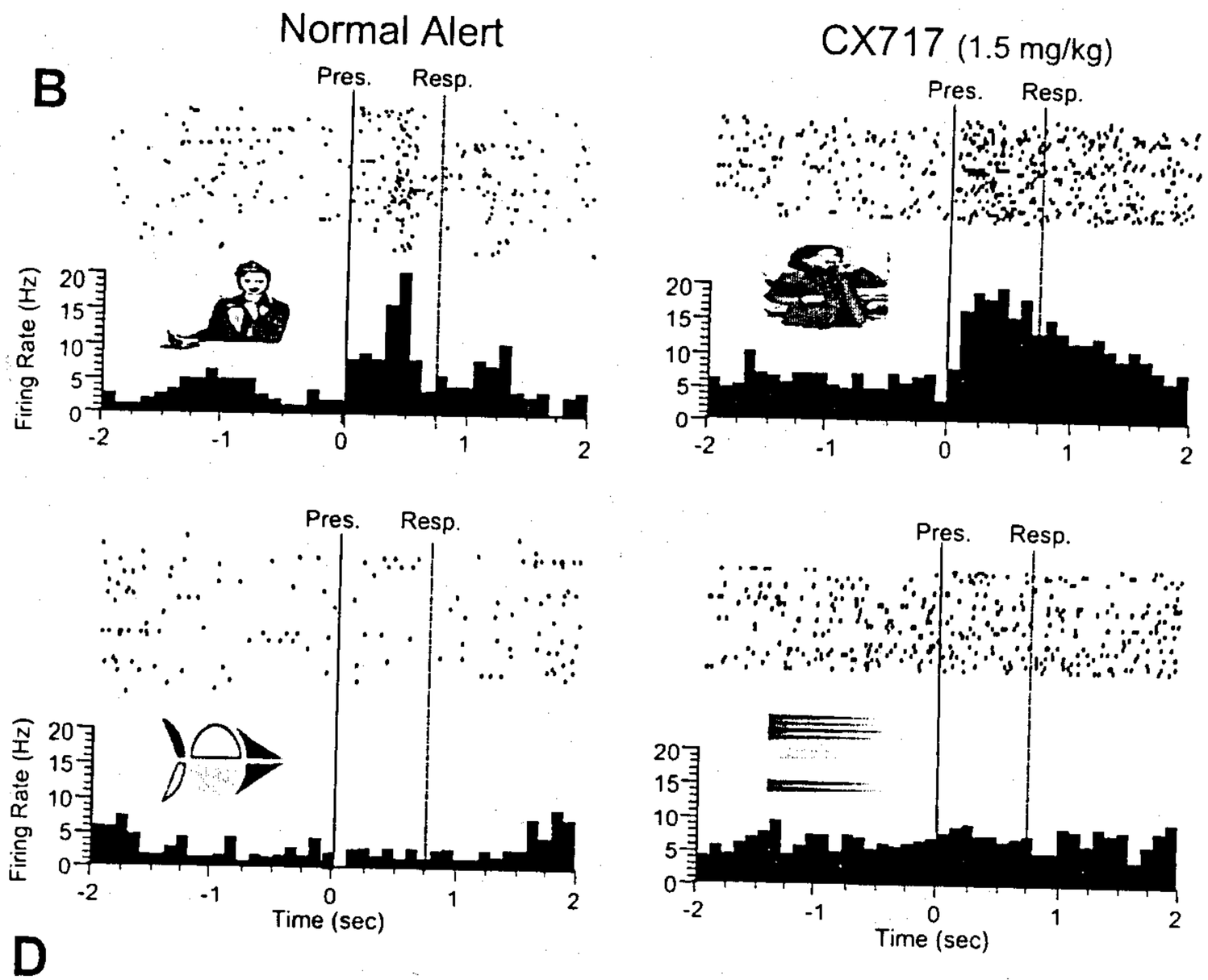
B
Normal Alert
CX717 (1.5 mg/kg)
Pres.
Resp.
Firing Rate (Hz)
Time (sec)

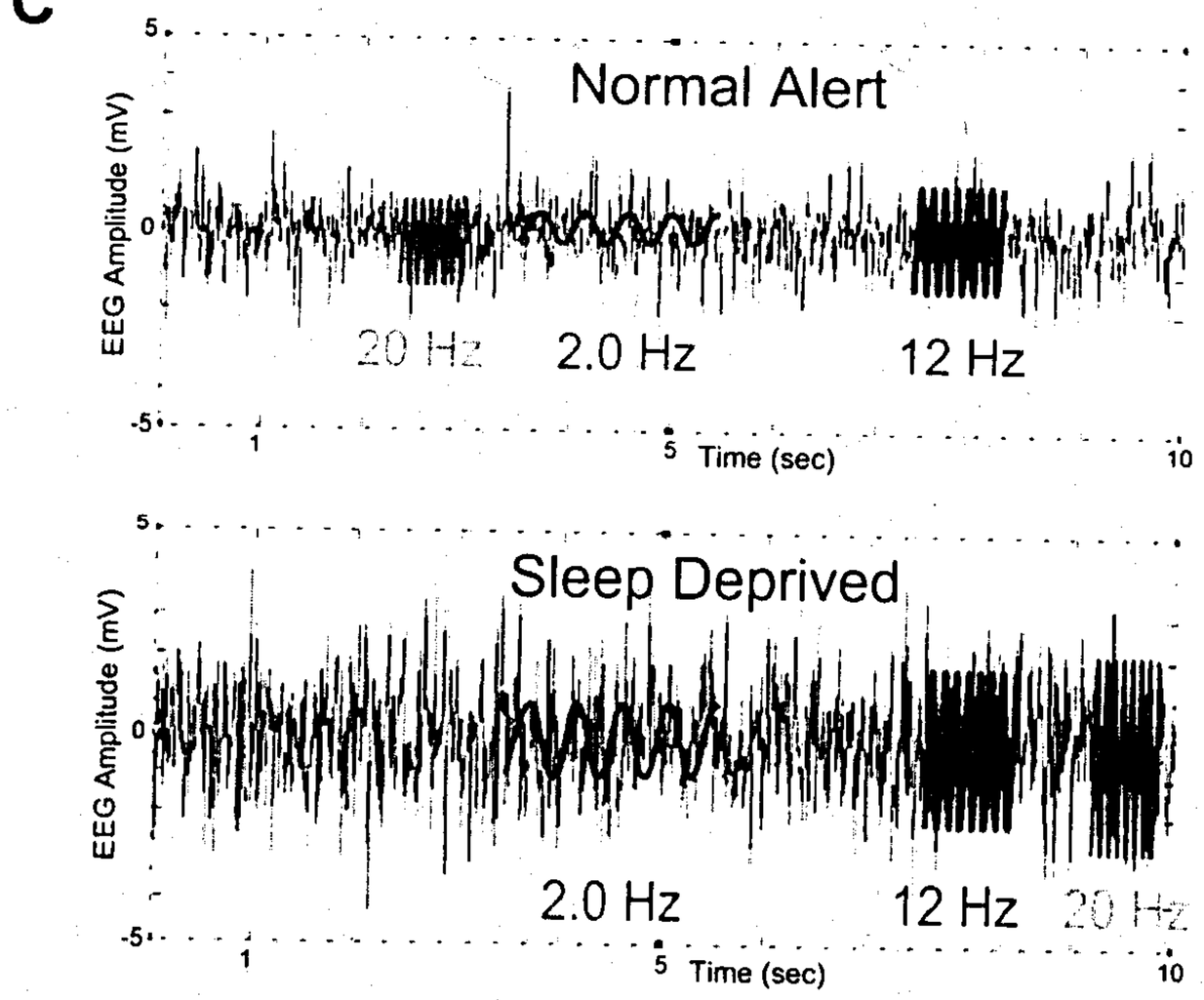
C
Normal Alert
EEG Amplitude (mV)
20 Hz
2.0 Hz
12 Hz
Time (sec)
Sleep Deprived
2.0 Hz
12 Hz
20 Hz

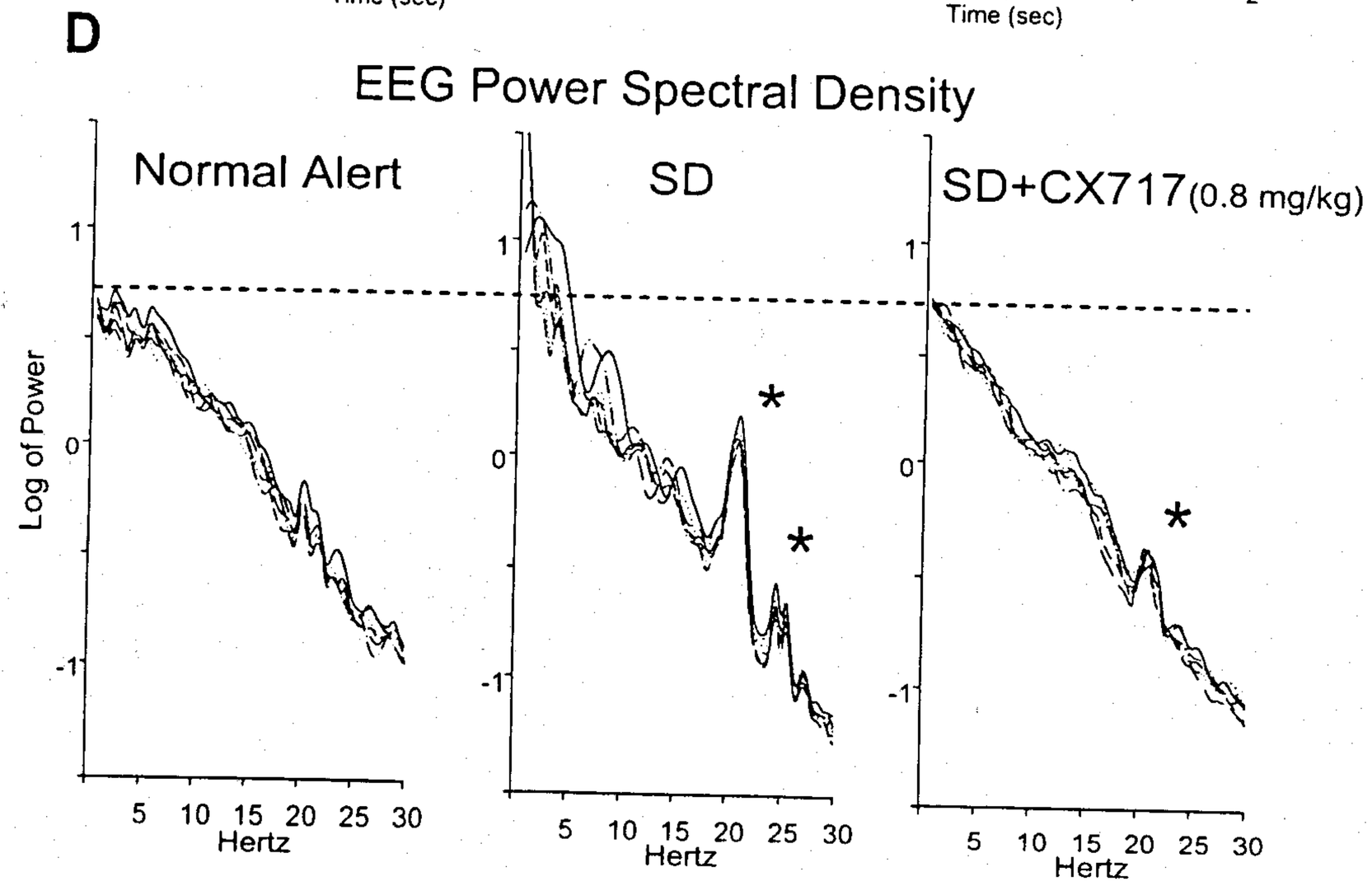
D
EEG Power Spectral Density
Normal Alert
SD
SD+CX717(0.8 mg/kg)
Log of Power
Hertz
*

Fig 5

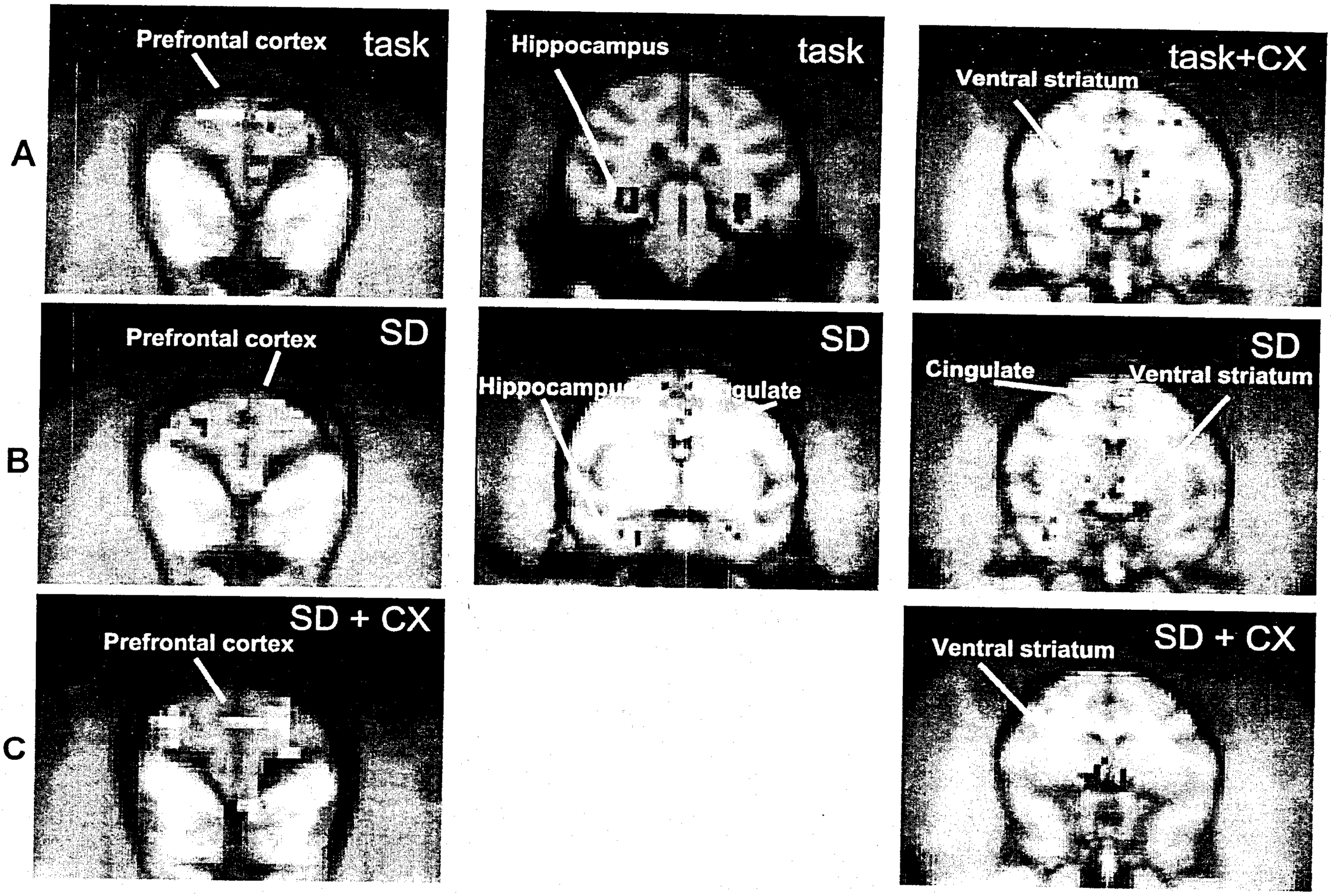
A
Prefrontal cortex
task
Hippocampus
task
task+CX
Ventral striatum
B
Prefrontal cortex
SD
SD
Cingulate
Ventral striatum
C
SD + CX
Prefrontal cortex
SD + CX
Ventral striatum

Fig 6

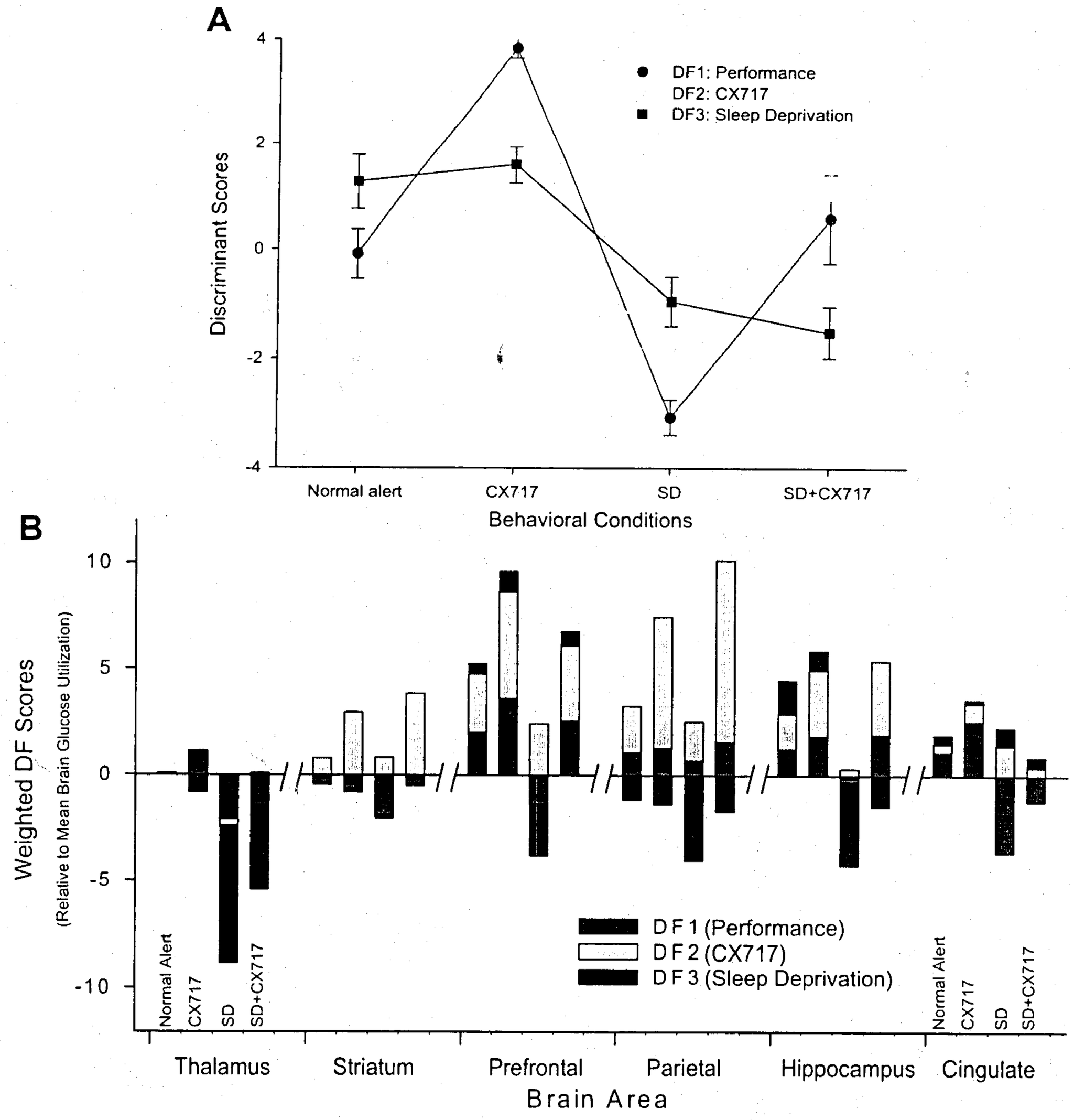
A
Discriminant Scores
4
2
0
-2
-4
DF1: Performance
DF2: CX717
DF3: Sleep Deprivation
Normal alert
CX717
SD
SD+CX717
Behavioral Conditions
B
Weighted DF Scores
(Relative to Mean Brain Glucose Utilization)
10
5
0
-5
-10
Normal Alert
CX717
SD
SD+CX717
DF 1 (Performance)
DF 2 (CX717)
DF 3 (Sleep Deprivation)
Thalamus
Striatum
Prefrontal
Parietal
Hippocampus
Cingulate
Brain Area

Table 1

Coordinates, cluster size and peak t-values of altered $lCMR_{glc}$ during DMS performance

		Normal rest										Sleep deprivation									
		Vehicle					CX717					Vehicle					CX717 (relative to SD-Veh)				
Regions		Size	Coordinate			t-value	Size	Coordinate			t-value	Size	Coordinate			t-value	Size	Coordinate			t-value
Prefrontal cortex	L	40	3	36	10	4.01						60	2	36	10	3.47	84	8	36	6	3.47
Prefrontal cortex	R	17	-12	36	8	3.76	56	-6	38	6	3.2	8	-14	32	10	2.96	54	-12	34	8	3.67
Hippocampus	L	8	8	4	-6	2.58	13	15	16	-18	3.3	127	12	16	-16	3.3					
Hippocampus	R	31	-6	2	-10	3.86	19	-10	16	-18	3.24										
Dorsal striatum	L																				
Dorsal striatum	R	10	-2	26	0	3.34						28	-8	22	4	3.17	25	-6	22	4	3.46
Ventral striatum	L						7	6	24	-6	2.91	24	4	26	-6	3.94	14	4	28	-6	3.07
Ventral striatum	R						10	-8	22	-8	2.83	15	-8	22	-10	3.89					
Sup temporal gyrus	L	21	18	0	-4	3.45															
Sup temporal gyrus	R																14	22	22	-4	4.83
Cingulate cortex	L						68	-2	20	8	4.53	69	0	12	16	5.15					
Cingulate cortex	R																				
Parietal cortex	L						31	8	4	14	3.58										
Parietal cortex	R						47	-18	14	0	5.02						53	-8	8	12	2.7
Thalamus	L											116	8	12	-4	3.52					
Thalamus	R																				
Visual cortex	L																				
Visual cortex	R						18	-12	-18	4	3.92	255	-20	-4	-10	4.87					

☐ Decreases